

Supplementary Materials: Interface-Controlled Pd Nanodot-Au Nanoparticle Colloids for Efficient Visible-Light-Induced Photocatalytic Suzuki-Miyaura Coupling Reaction

Eunmi Kang, Hyeon Ho Shin and Dong-Kwon Lim *

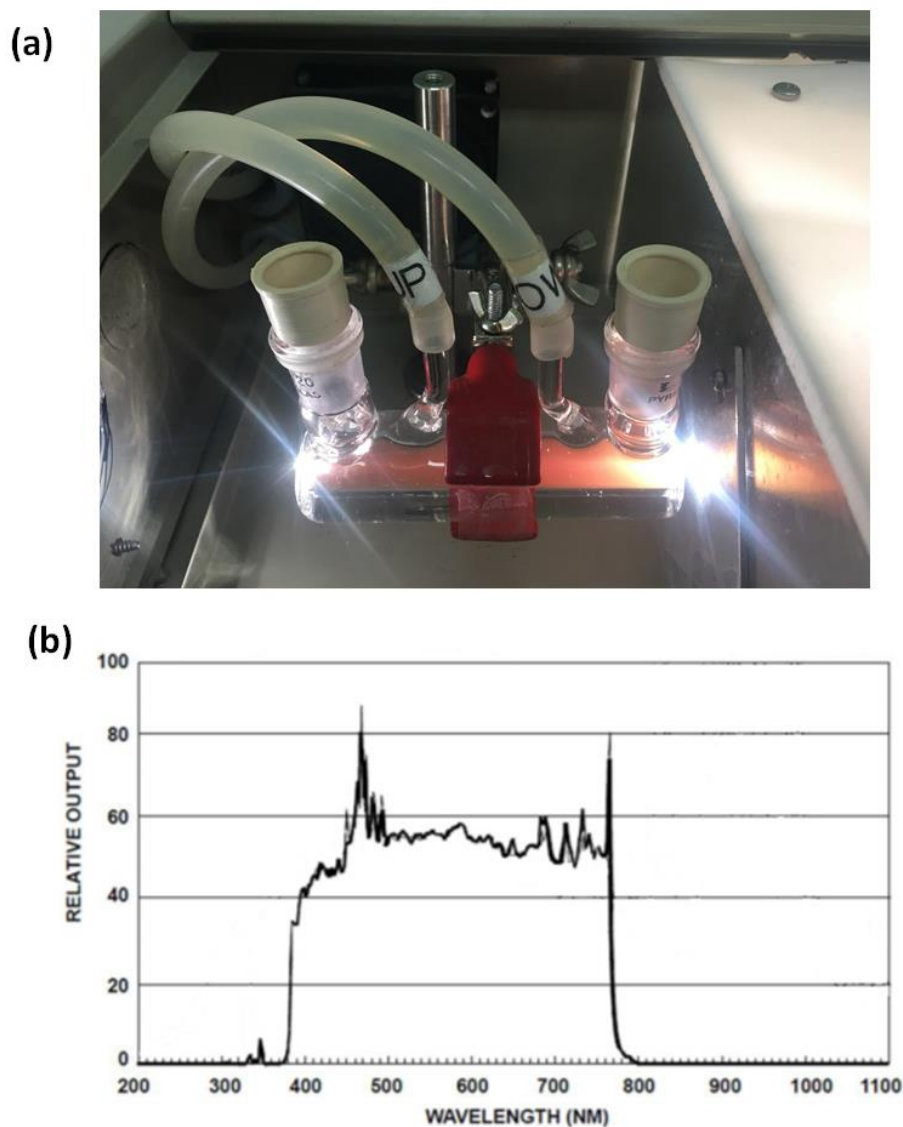


Figure S1. Instrumental setup for the Suzuki-Miyaura coupling reaction. (a) Light from the Xe lamp (400–780 nm) illuminates the reactor (Pyrex, 15 mL) equipped with a water circulation jacket. (b) The emission profiles of Xe-lamp used in this experiment.

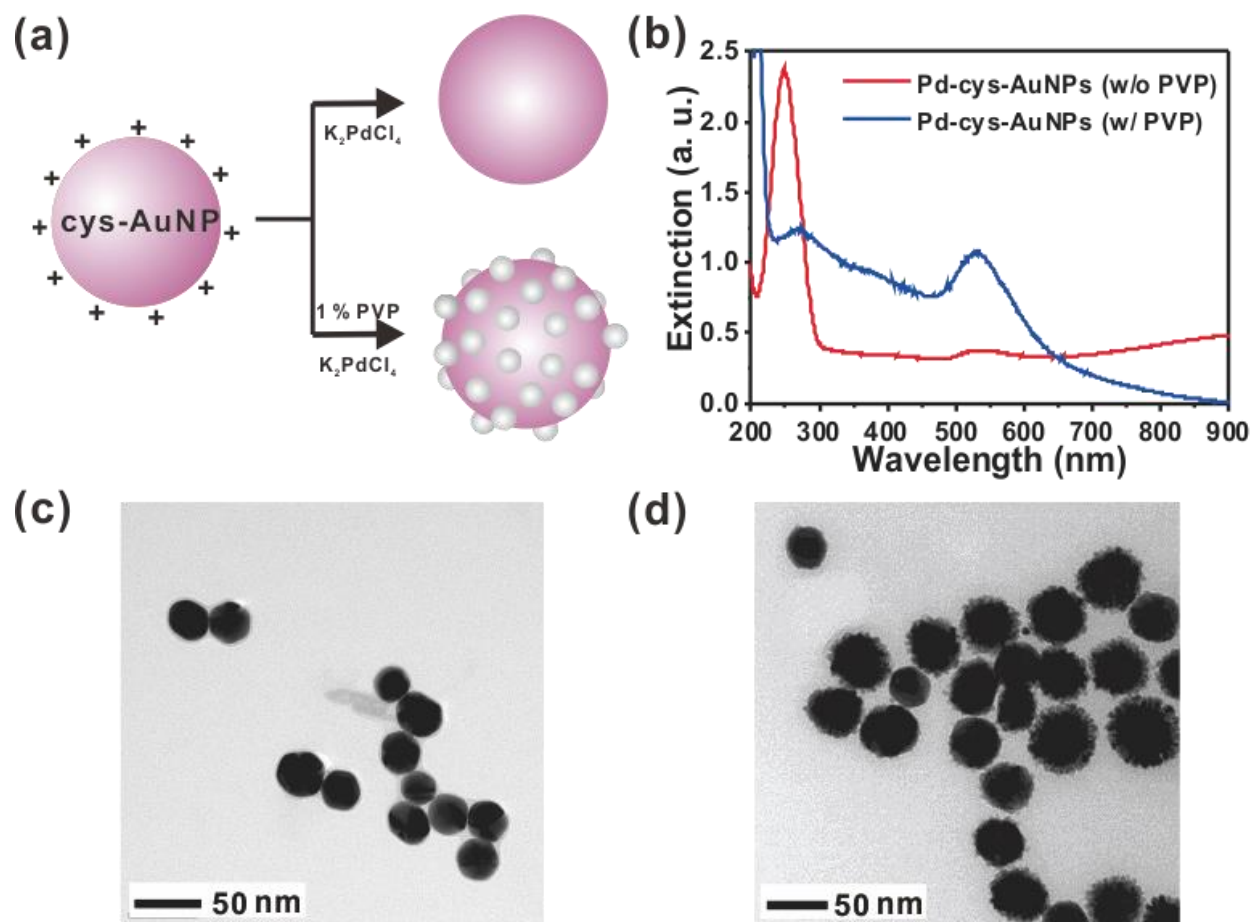


Figure S2. (a) Preparation of Pd-nanodot-decorated AuNPs using cysteamine-modified AuNPs with or without 1% PVP, (b) UV-Vis spectra of Pd-cys-AuNPs prepared with (blue-line) or without PVP (red-line), (c) TEM images of the nanoparticles prepared without 1% PVP, (d) TEM images of the nanoparticles prepared with 1% PVP.

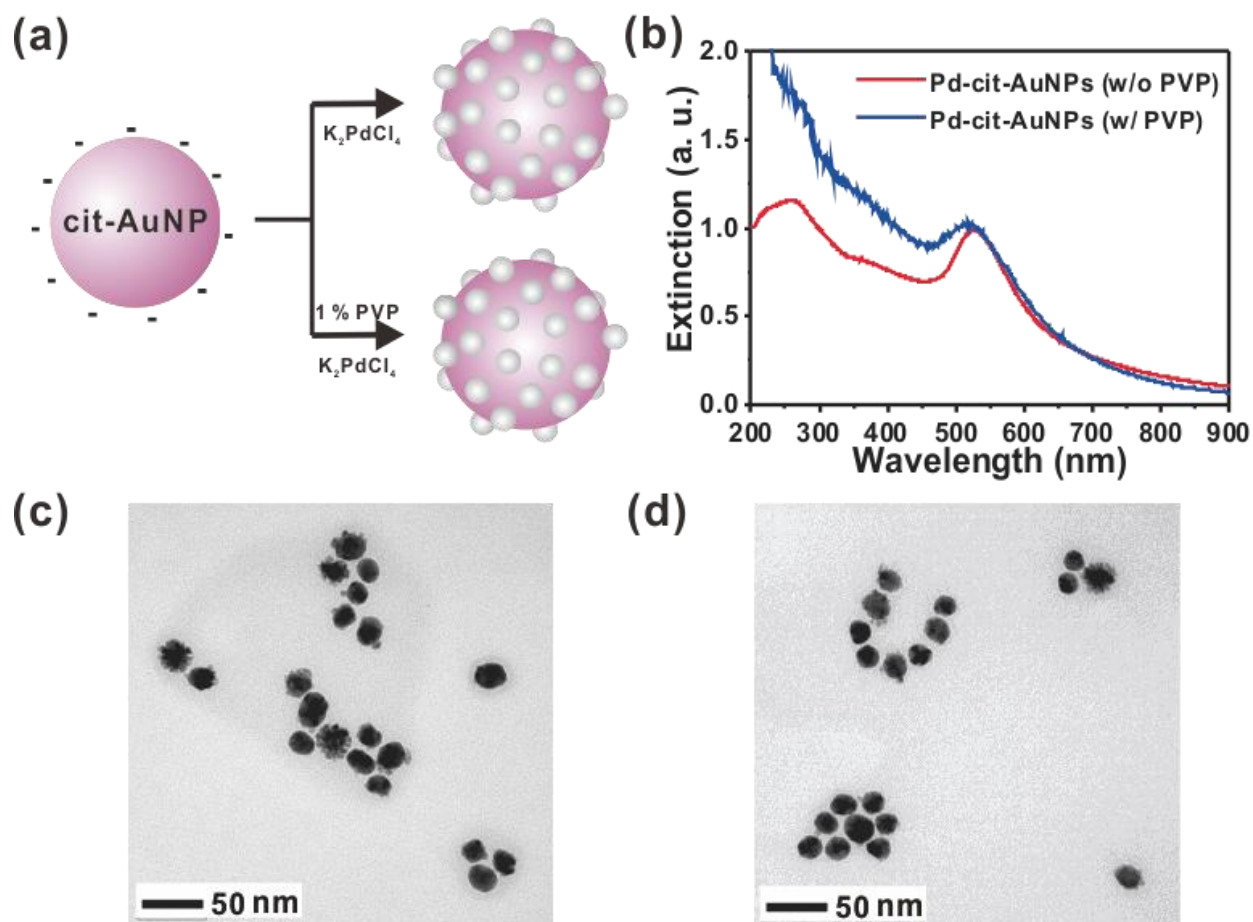


Figure S3. (a) Preparation of Pd-nanodot-decorated AuNPs using citrate-modified AuNPs with or without 1% PVP, (b) UV-Vis spectra of Pd-citrate-AuNPs prepared with (blue-line) or without PVP (red-line), (c) TEM images of the nanoparticles prepared without 1% PVP, (d) TEM images of the nanoparticles prepared with 1% PVP.

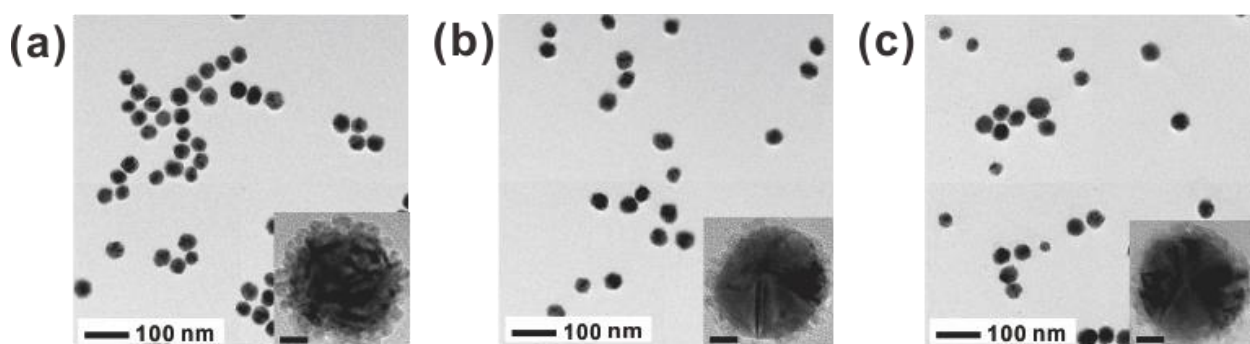


Figure S4. TEM images of (a) Pd-cys-AuNPs, (b) Pd-GO-AuNPs, and (c) Pd-rGO-AuNPs (Scale bar in the inset is 10 nm).

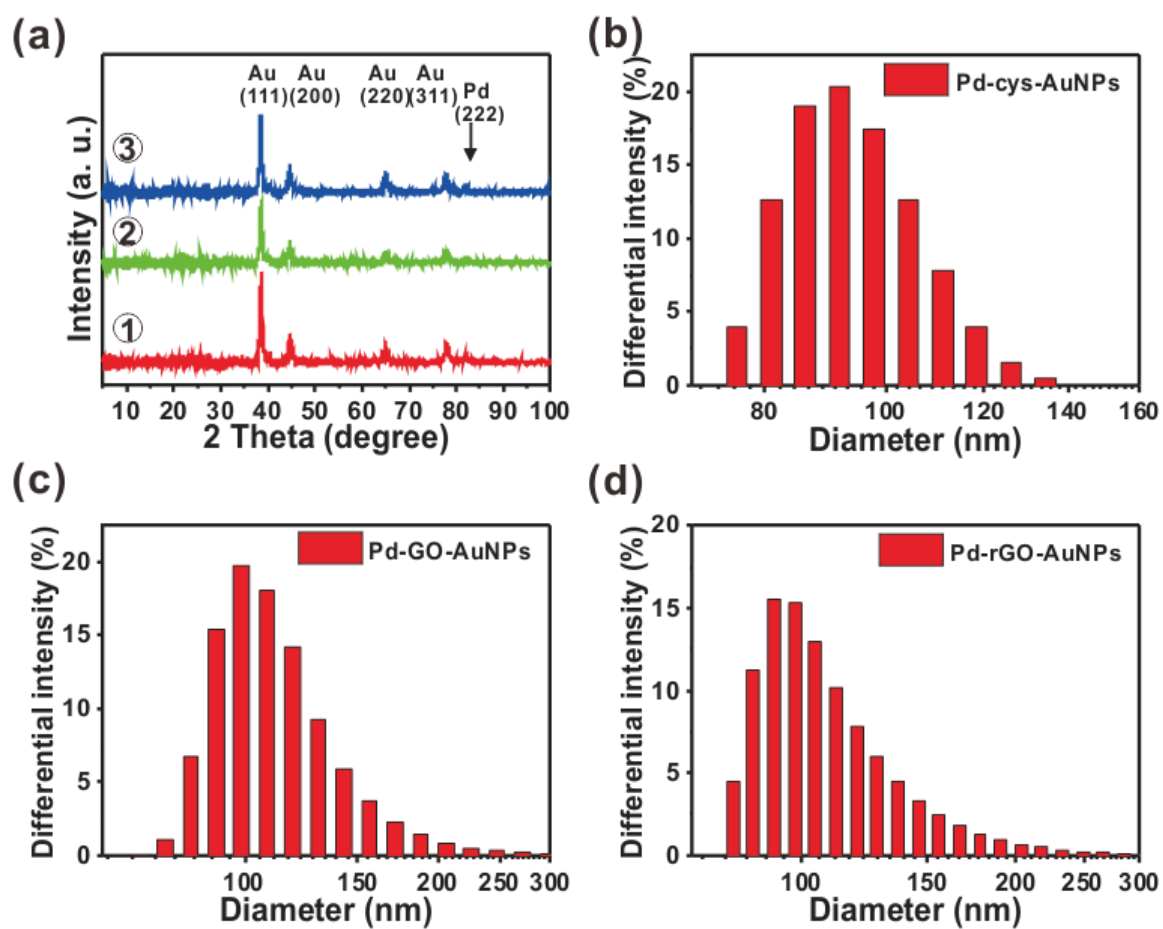


Figure S5. (a) XRD spectra and size distribution of (b) Pd-cys-AuNPs, (c) Pd-GO-AuNPs, and (d) Pd-rGO-AuNPs.

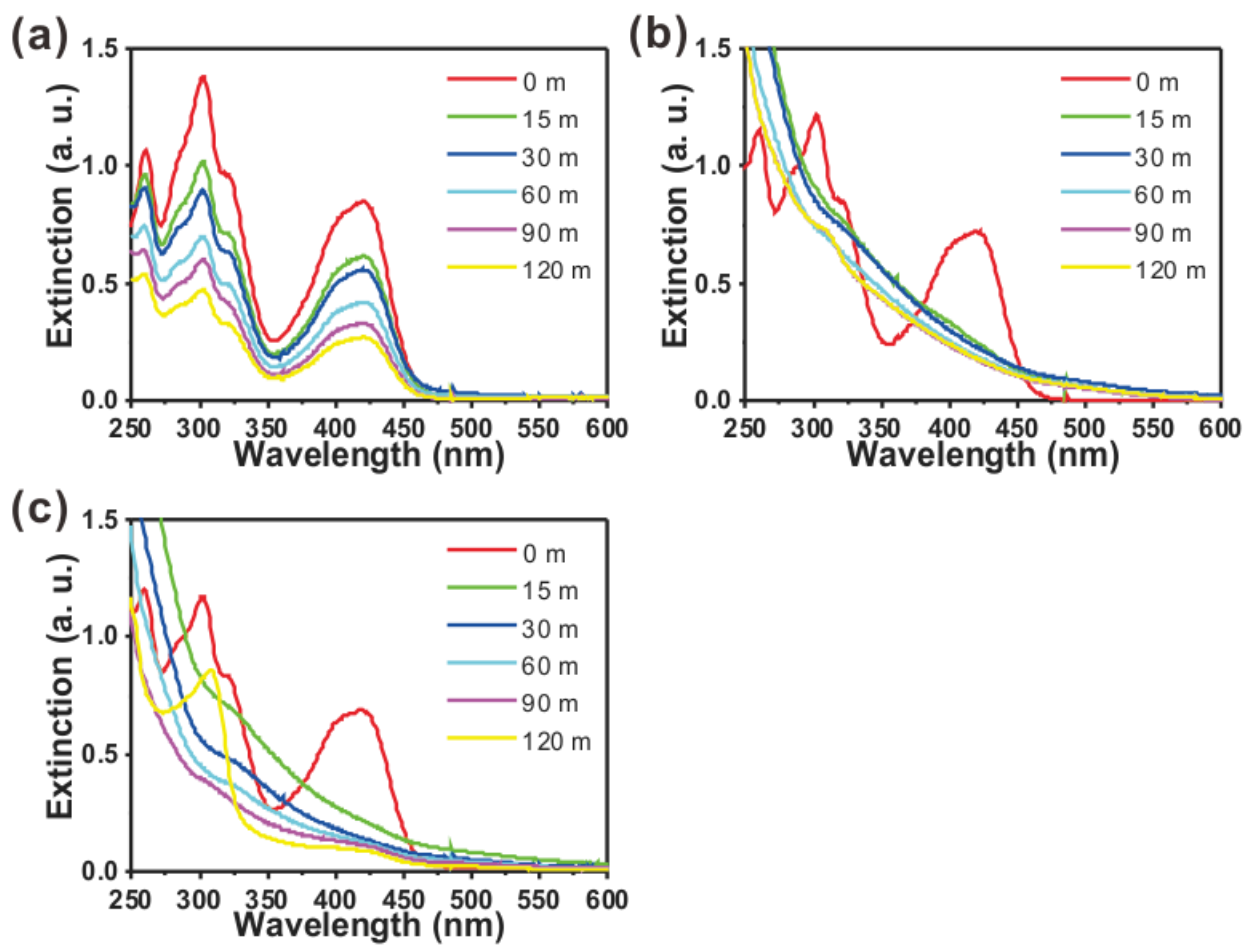


Figure S6. Time dependent reduction of Fe^{3+} to Fe^{2+} in the presence of (a) Pd-cys-AuNPs, (b) Pd-GO-AuNPs, and (c) Pd-rGO-AuNPs with Xe lamp illumination.

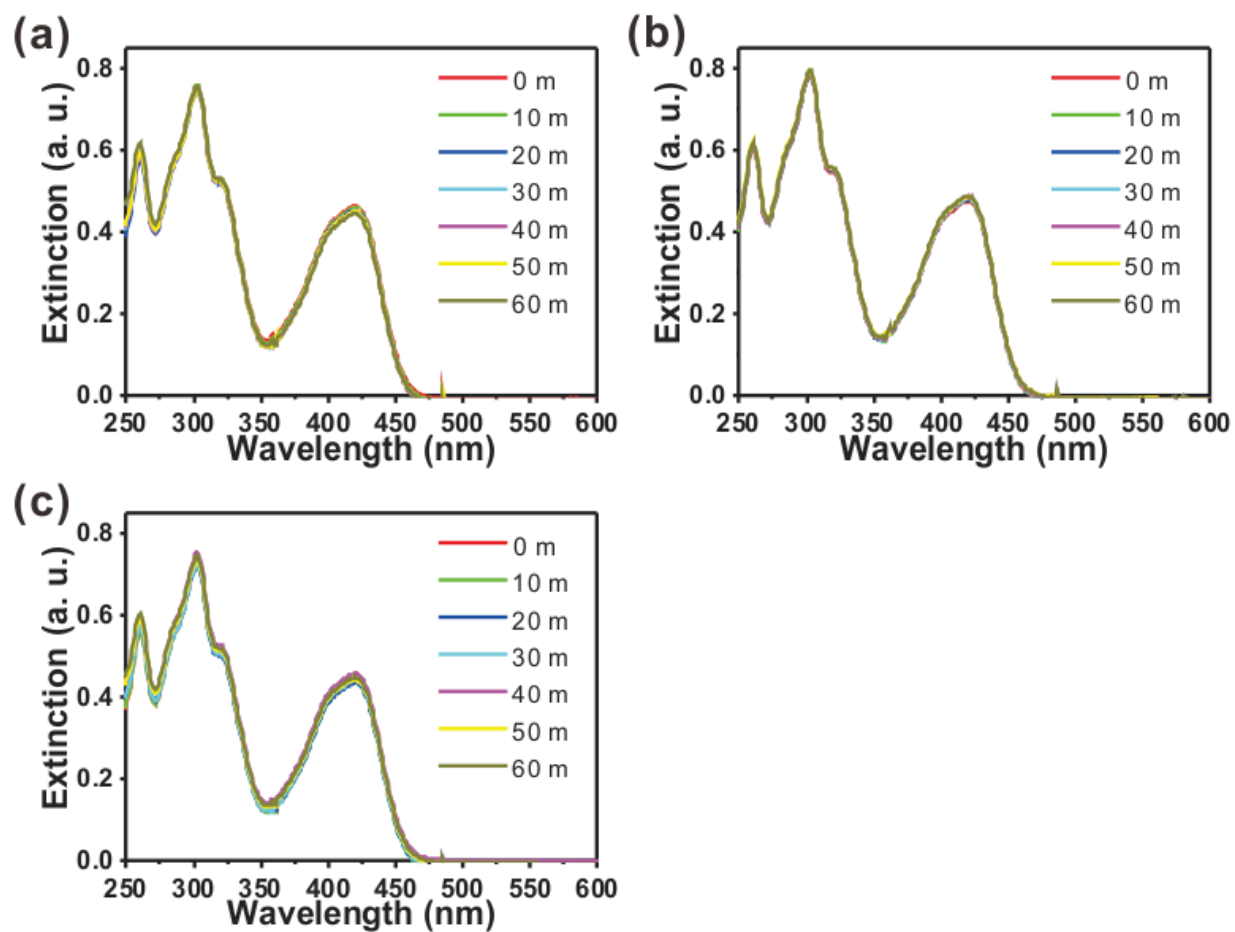


Figure S7. Time dependent reduction of Fe³⁺ to Fe²⁺ in the presence of (a) Pd-cys-AuNPs, (b) Pd-GO-AuNPs, and (c) Pd-rGO-AuNPs with NIR laser.

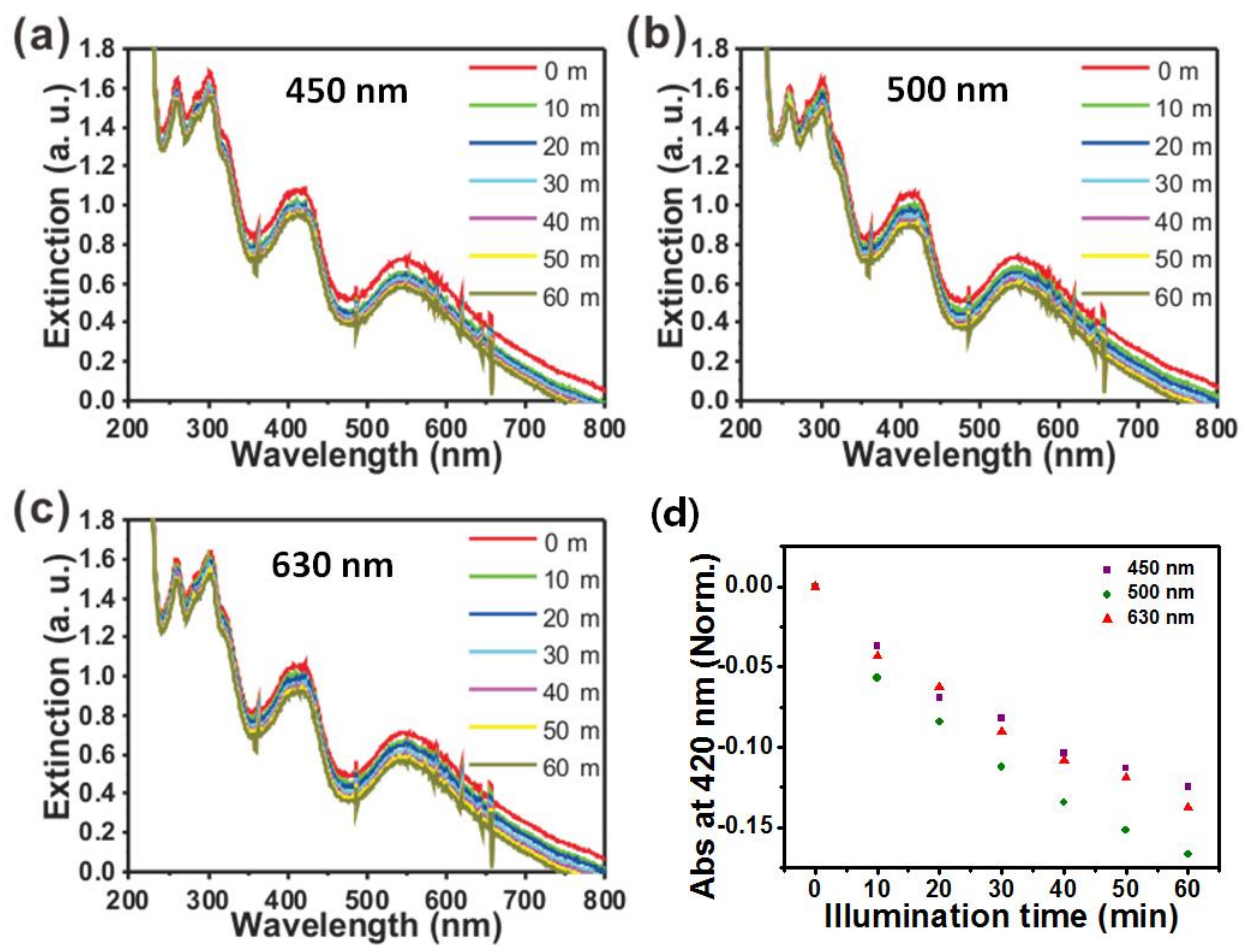
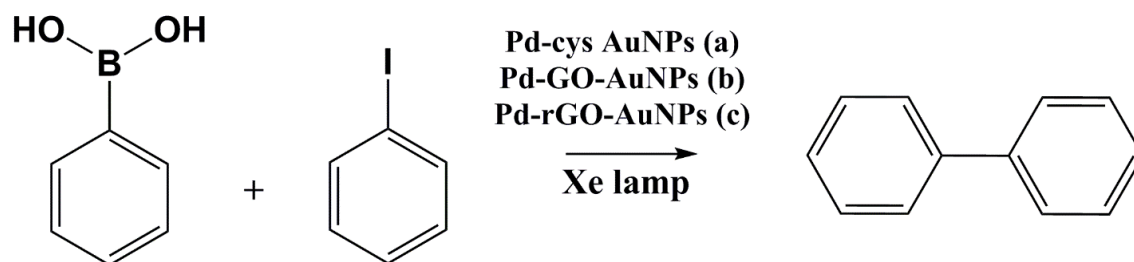


Figure S8. Wavelength dependent reduction of Fe³⁺ to Fe²⁺ in the presence of Pd-rGO-AuNPs with Xe lamp illumination and band-pass filter (450, 500, and 650 nm).



Entry	Catalyst	Light source	Power (W/cm ²)	Temperature (initial/final, °C)	Yield* (%)	Conversion (%)
1	a	Xe	5.24	25/50	29.8	45.1
2	b	Xe	5.24	25/51	56.0	62.7
3	c	Xe	5.24	25/52	66.4	70.6
4	a	Xe	5.24	25/25	6.7	31.1
5	b	Xe	5.24	25/25	30.9	36.8
6	c	Xe	5.24	25/25	55.6	40.8

* Analytical yield is calculated based on the HPLC analysis and calibration curve.

$$* \text{ Conversion\%} = \frac{\text{Initial area of Iodobenzene} - \text{Final area of Iodobenzene}}{\text{Initial area of Iodobenzene}} \times 100$$

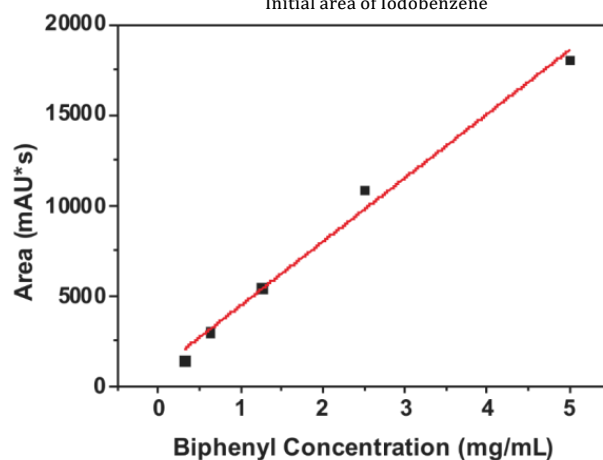


Figure S9. Results of photocatalytic reactions performed in the presence of (a) Pd-cys AuNPs, (b) Pd-GO-AuNPs, or (c) Pd-rGO-AuNPs at uncontrolled temperature (Entry 1,2,3) or at controlled temperature (25 °C) (Entry 4,5,6) and calibration curve for biphenyl product.

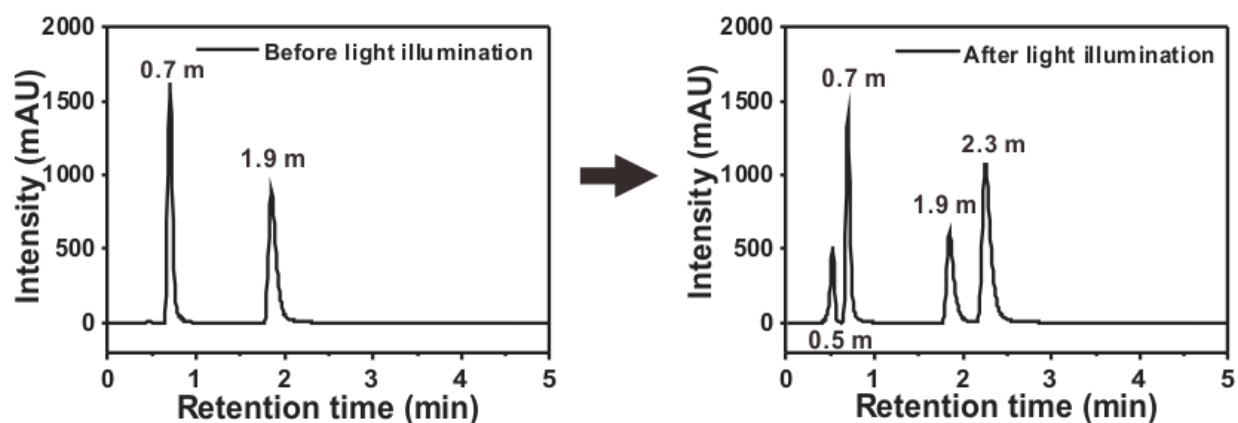


Figure S10. The representative chromatogram of the Suzuki-coupling reaction (Retention time: by product - 0.5 min, phenyl boronic acid - 0.7 min, iodobenzene - 1.9 min, biphenyl (product) - 2.3 min).

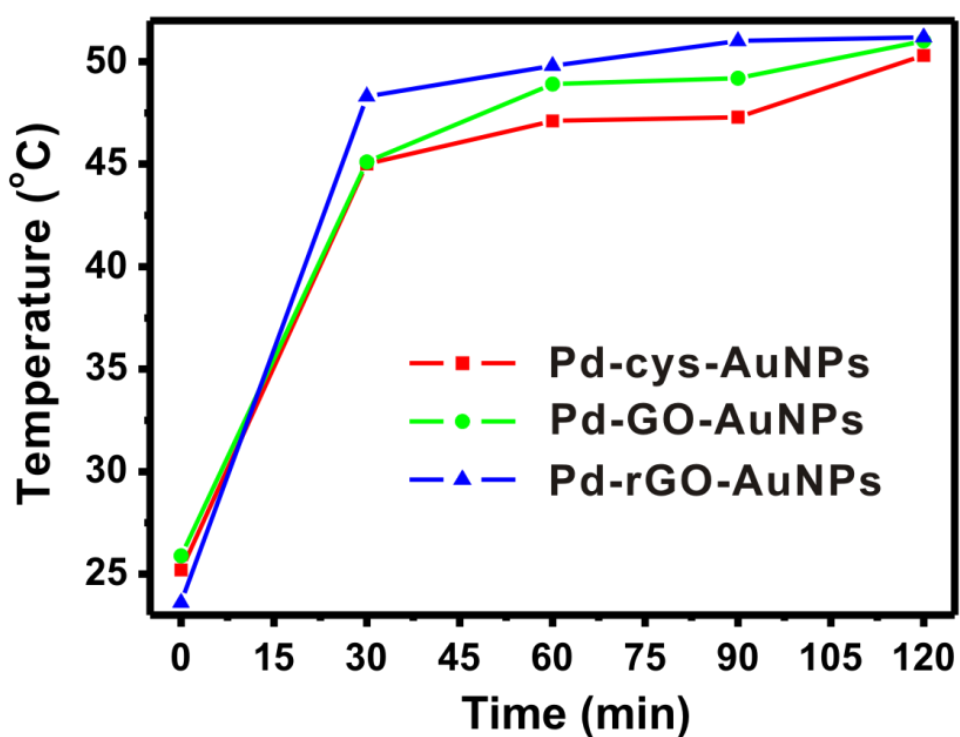


Figure S11. Temperature changes of reaction mixtures during the coupling reactions with light illumination in the presence of Pd-cys-AuNPs, Pd-GO-AuNPs, and Pd-rGO-AuNPs.

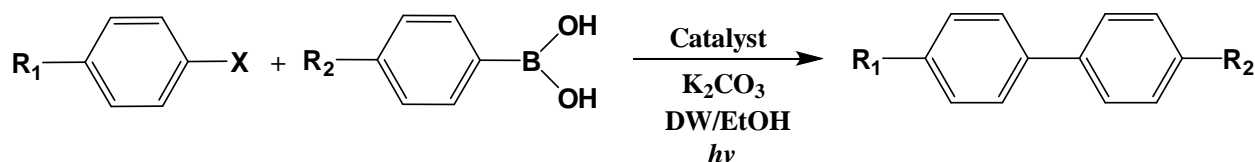


Figure S12. The summary of coupling reaction with various haloarens and substituted phenylboronic acids in the presence of Pd rGO-AuNPs with light illumination.

Entry	X	R1	R2	Conversion (%)	Selectivity (%)
1	I	H	H	98.1	99.5
2	I	H	CH3	99.2	95.3
3	I	CH3	H	94.2	96.5
4	Br	H	H	75.5	>99.9
5	Cl	H	H	31.1	>99.9

*Reaction condition: The Pd-rGO-AuNP solution (OD 0.4 at 540 nm, 5.0 mL) was mixed with phenylboronic acid (97.6 mg, 0.8 mmol), ethanol (6.25 mL), iodobenzene (44.5 μL , 0.4 mmol), and K_2CO_3 (1.25 mL, 1 mmol). Xe-lamp light illuminated to the reactor without controlling the reaction temperature and analysed the reaction mixtures with HPLC and determined the yield and impurity.

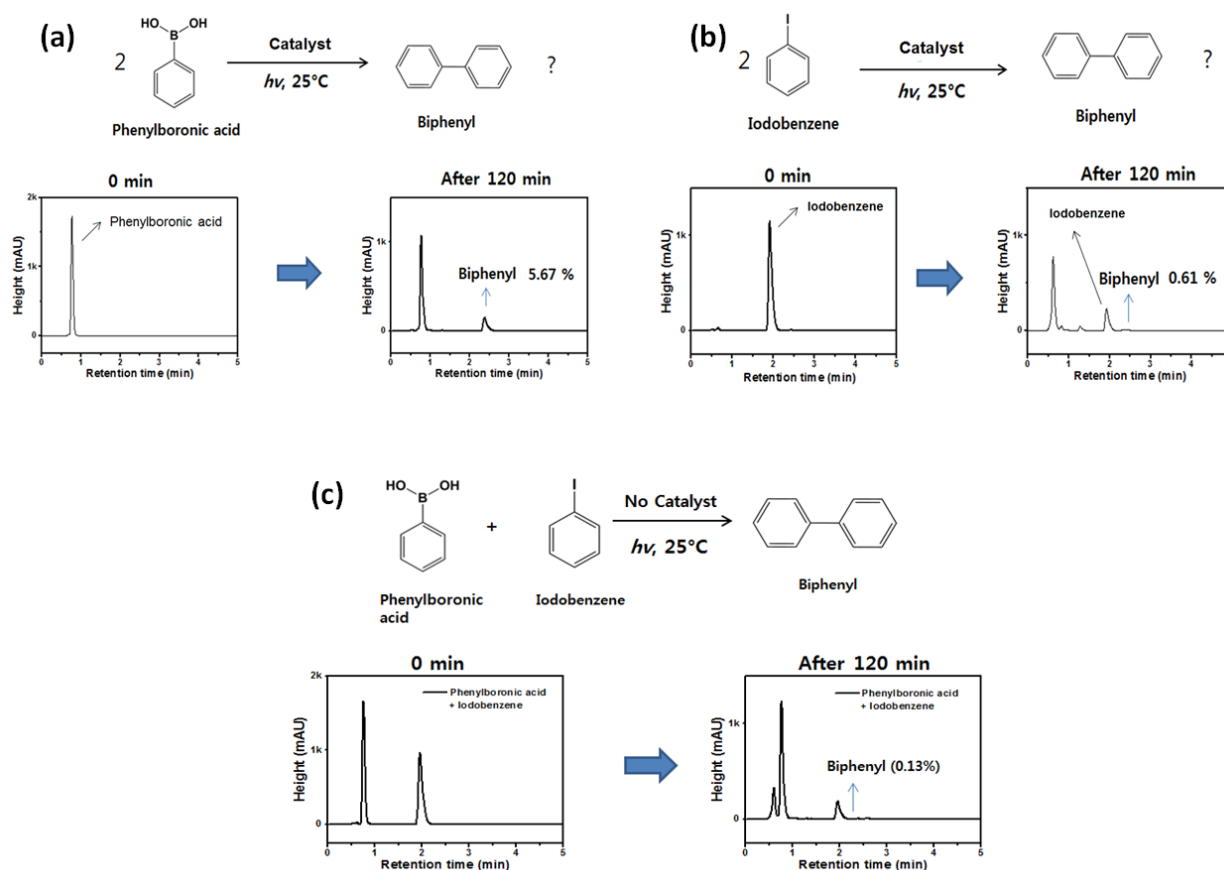


Figure S13. The results of self-coupling reaction with phenylboronic acid (a) or iodobenzene (b) in the presence of Pd rGO-AuNPs with light illumination. The visible light induced reaction without Pd rGO-AuNPs catalyst (c).

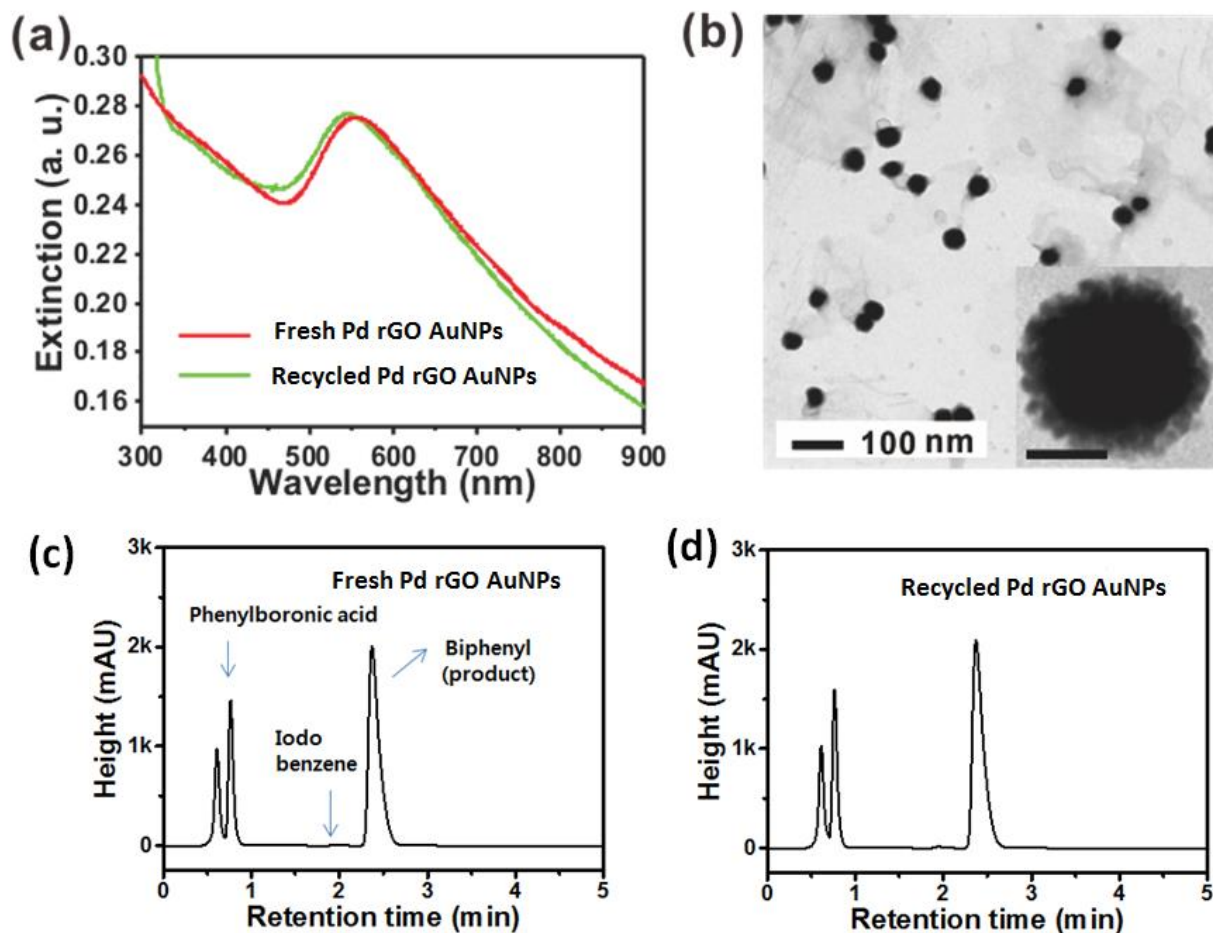


Figure S14. Comparison of Pd-rGO-AuNPs before and after the Suzuki-Miyaura coupling reaction. (a) UV-Vis spectra of Pd-rGO-AuNPs before (red line) and after reaction (green line), (b) TEM image of Pd-rGO-AuNPs after reaction (Scale bar in the inset is 20 nm). (c) The chromatogram of reaction mixtures after completion of reaction using fresh Pd rGO-AuNP catalyst. (d) The chromatogram of reaction mixtures after completion of reaction using recycled Pd rGO-AuNP catalyst.